



The microRNAs *let-7* and *miR-9* down-regulate the axon-guidance genes *Ntn1* and *Dcc* during peripheral nerve regeneration

Received for publication, January 2, 2019 Published, Papers in Press, January 9, 2019, DOI 10.1074/jbc.RA119.007389

Xinghui Wang¹, Qianqian Chen¹, Sheng Yi, Qianyan Liu, Ruirui Zhang, Pan Wang, Tianmei Qian, and Shiyong Li²

From the Key Laboratory of Neuroregeneration of Jiangsu and Ministry of Education, Co-innovation Center of Neuroregeneration, Nantong University, Nanjing, Jiangsu 226001, China

Edited by Ronald C. Wek

Axon guidance helps growing neural axons to follow precise paths to reach their target locations. It is a critical step for both the formation and regeneration of neuronal circuitry. Netrin-1 (Ntn1) and its receptor, deleted in colorectal carcinoma (Dcc) are essential factors for axon guidance, but their regulation in this process is incompletely understood. In this study, using quantitative real-time RT-PCR (qRT-PCR) and biochemical and reporter gene assays, we found that the *Ntn1* and *Dcc* genes are both robustly up-regulated in the sciatic nerve stump after peripheral nerve injury. Moreover, we found that the microRNA (miR) *let-7* directly targets the *Ntn1* transcript by binding to its 3'-untranslated region (3'-UTR), represses Ntn1 expression, and reduces the secretion of Ntn1 protein in Schwann cells. We also identified *miR-9* as the regulatory miRNA that directly targets *Dcc* and found that *miR-9* down-regulates *Dcc* expression and suppresses the migration ability of Schwann cells by regulating *Dcc* abundance. Functional examination in dorsal root ganglion neurons disclosed that *let-7* and *miR-9* decrease the protein levels of Ntn1 and *Dcc* in these neurons, respectively, and reduce axon outgrowth. Moreover, we identified a potential regulatory network comprising *let-7*, *miR-9*, Ntn1, *Dcc*, and related molecules, including the RNA-binding protein Lin-28 homolog A (Lin28), SRC proto-oncogene nonreceptor tyrosine kinase (Src), and the transcription factor NF- κ B. In summary, our findings reveal that the miRs *let-7* and *miR-9* are involved in regulating neuron pathfinding and extend our understanding of the regulatory pathways active during peripheral nerve regeneration.

Peripheral nerve injury is common in clinical cases and affects the patients' quality of life severely (1–3). Thus, investigating the molecular mechanisms underlying the peripheral nerve regeneration for the development of medical therapies is

This work was supported by National Key R&D Program of China Grant 2017YFA0104703, National Key Research and Development Program of China Grant 31730031, Collegiate Natural Science Fund of Jiangsu Province Grant 16KJA310005, the Priority Academic Program Development of Jiangsu Higher Education Institutions (PAPD), Natural Science Foundation of Nantong Grant MS12017015-2, and Postgraduate Research & Practice Innovation Program of Jiangsu Province Grant KYCX18-2398. The authors declare that they have no conflicts of interest with the contents of this article.

¹ Both authors contributed equally to this work.

² To whom correspondence should be addressed. E-mail: lisy0379@ntu.edu.cn.

critical. Neurons extend axons such that, they reach their targets precisely by navigating through a complex regeneration microenvironment with an extreme precision process known as axon guidance during nerve repair and regeneration (4, 5). It is essential for axons to target their destinations precisely for functional recovery.

In recent years, microRNAs (miRNAs)³ are a class of small noncoding RNAs that have emerged, as key post-transcriptional regulators in a majority of the eukaryotic cells (6, 7). In animals, miRNAs bind to partially complementary sites in mRNAs, leading to translational repression and mRNA deadenylation and degradation (8–10). Previously, we identified a series of differentially expressed miRNAs and found that these miRNAs affect the microenvironment after peripheral nerve regeneration (11–15). Debris removal, axonal growth, and axon guidance are key elements that affect the regenerative microenvironment and contribute to peripheral nerve regeneration. Our previous studies showed that after sciatic nerve injury, *let-7* and *miR-1* regulate the phenotype of SCs by directly targeting the nerve growth factors, NGF and BDNF separately, and further promoting the axon growth of sciatic nerve (12, 13). In addition, we found that *miR-340* could target and regulate the tPA for debris clearance and axon growth (14). In the current study, we explored the regulation mechanism of axon guidance during peripheral nerve regeneration.

Netrin-1 (Ntn1) is overexpressed in many cancer tissues. A decreased expression of Ntn1 or inhibition of Ntn1 receptor expression might induce apoptosis in tumor cells and lead to tumor regression (16, 17). Moreover, Ntn1 is one of the most studied axon guidance factors. It builds the neural conduction pathways and directs the migration of neuronal cells (18). According to the expressions of netrin receptors, Ntn1 attracts and repels the motor axons in distinct populations (19). Deleted in colorectal carcinoma (Dcc) is one of the major receptors of Ntn1 (20). Ntn1 binds to Dcc, mediates its axon guidance, and guides the axonal growth and directional cell migration (21–23). It has also been demon-

³ The abbreviations used are: miRNA, microRNA; SC, Schwann cell; NGF, nerve growth factor; BDNF, brain-derived neurotrophic factor; Ntn1, Netrin-1; Dcc, deleted in colorectal carcinoma; qRT, quantitative real-time; DMEM, Dulbecco's modified Eagle's medium; DRG, dorsal root ganglion; GAPDH, glyceraldehyde-3-phosphate dehydrogenase; tPA, tissue plasminogen activator.

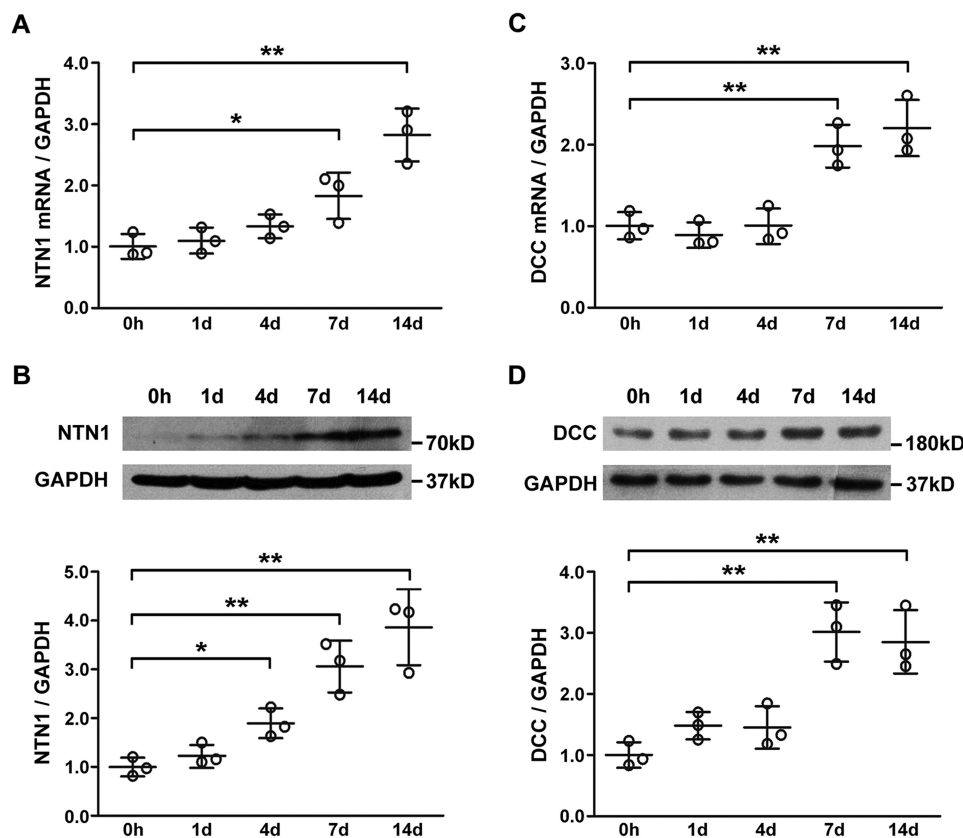


Figure 1. The temporal expression patterns of *Ntn1* and *Dcc* in the injured nerve stumps after sciatic nerve injury. A and C, the mRNA expressions of *Ntn1* and *Dcc*, and B and D, the protein expressions of *Ntn1* and *Dcc* in the sciatic nerve stumps after crush were determined by qRT-PCR and Western blot analysis, respectively ($n = 3/\text{group}$). *Gapdh* was used as a loading control. *, $p < 0.05$ and **, $p < 0.01$ versus 0 h control.

stated that the expression levels of *Ntn1* and *Dcc* increased significantly during sciatic nerve autoimmune inflammation. The elevated levels of *Ntn1* and *Dcc* promote cell survival and axon regeneration (24). These studies imply that *Ntn1* and *Dcc* might play critical roles in promoting axon growth and guiding axons to their final destinations during peripheral nerve regeneration.

Following peripheral nerve injury, the expression levels of several genes are altered and these genes affect the biological behaviors of neurons and SCs (5, 25–27). Emerging studies have showed that miRNAs are critical fine-tuning regulatory molecules in axon guidance (4, 28, 29). Because the regulatory mechanisms of *Ntn1* and *Dcc* are yet incomprehensive, our current study aims to investigate the regulatory mechanisms and roles of miRNAs on *Ntn1* and *Dcc*.

Results

Ntn1 and *Dcc* expressions were elevated after sciatic nerve injury

Quantitative real time-PCR (qRT-PCR) analysis showed that the mRNA expressions of *Ntn1* in the sciatic nerve stumps after nerve crush was increased from day 1 after nerve injury as compared with 0 h after nerve injury, and significantly increased at days 7 and 14 after nerve injury (Fig. 1A). Western blot analysis showed that the protein expressions of *Ntn1* in the crushed nerve stumps were also increased from day 1 after nerve injury as compared with the

0-h control, and significantly increased at days 4, 7, and 14 (Fig. 1B). Detailed analysis displayed that at day 4 post-nerve injury, expression of the *Ntn1* protein was significantly elevated as compared with that of the 0-h control, whereas the mRNA expression did not differ significantly (Fig. 1, A and B). Also, the mRNA and protein expressions of *Dcc* in the crushed nerve segments were increased after nerve crush, reaching a peak value at days 7 and 14 (Fig. 1, C and D). The protein expression of *Dcc* reached a peak value at day 7 post-injury, whereas the mRNA expression of *Dcc* did not reach a peak value until day 14 post-injury (Fig. 1, C and D).

let-7 negatively regulated *Ntn1* by directly targeting its 3'-UTR

The TargetScan prediction and the negative correlation between miRNA and mRNA expression patterns after sciatic nerve injury were demonstrated previously by microarray and Solexa sequencing (30, 31). A total of 9 miRNAs were identified as potential regulatory miRNAs of *Ntn1*, whereas 4 miRNAs, *let-7*, *miR-17*, *miR-27*, and *miR-128*, were conserved across species (Fig. 2A). These miRNAs were subjected to luciferase reporter assay to explore whether they could directly target *Ntn1*. The results suggested that only *let-7* could significantly decrease the luciferase activity (Fig. 2B). In addition, WT *Ntn1* or mutant 3'-UTR of the *let-7*-binding site was constructed and introduced into the downstream region of the luciferase gene (Fig. 2C). Co-transfection of the WT *Ntn1*-containing plasmid and *let-7* mimic

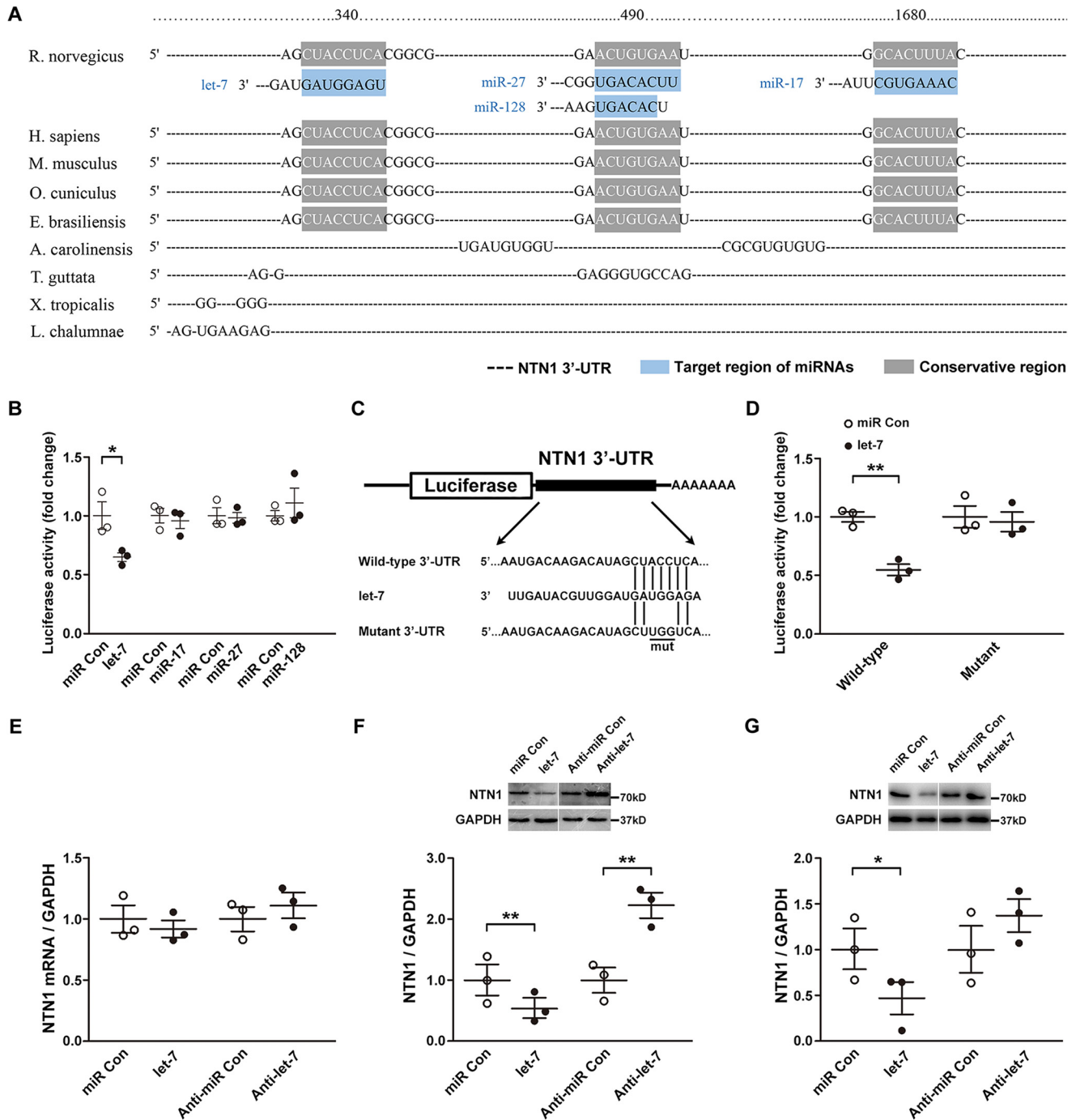


Figure 2. Identification of potential regulatory miRNAs targeting Ntn1. *A*, sequence alignment of the putative *let-7*-, *miR-17*-, *miR-27*-, and *miR-128*-binding sites across species. *B*, relative luciferase activities of 293T cells transfected with *let-7* mimic (*let-7*), *miR-17* mimic (*miR-17*), *miR-27* mimic (*miR-27*), *miR-128* mimic (*miR-128*), and mimic control (*miR Con*) ($n = 3$ /group). *C*, sketches of the construction of wild-type or mutant *p-Luc-UTR* vectors for *let-7*. *D*, the relative luciferase activities of 293T cells transfected with WT or mutant *p-Luc-UTR* and *let-7* mimic (*let-7*) or mimic control (*miR Con*) ($n = 3$ /group). *E*, the mRNA expressions of *Ntn1* in SCs transfected with *let-7* mimic (*let-7*) and mimic control (*miR Con*) or with *let-7* inhibitor (*Anti-let-7*) and inhibitor control (*Anti-miR Con*) ($n = 3$ /group). *F*, the expression of Ntn1 protein in SCs transfected with *let-7* mimic (*let-7*) and mimic control (*miR Con*) or with *let-7* inhibitor (*Anti-let-7*) and inhibitor control (*Anti-miR Con*) ($n = 3$ /group). *G*, the expression of Ntn1 protein in injured sciatic nerve stumps that were injected with a mixture containing *let-7* agomir (*let-7*) and agomir control (*miR Con*) or *let-7* antagonist (*Anti-let-7*) and antagonist control (*Anti-miR Con*), respectively ($n = 3$ /group). *, $p < 0.05$ and **, $p < 0.01$ versus control.

reduced luciferase activity, whereas mutant *Ntn1*-containing plasmid failed to show this effect (Fig. 2*D*), indicating that *let-7* directly bound to the 3'-UTR of *Ntn1*.

Furthermore, we observed the effects of *let-7* on the mRNA and protein abundances of Ntn1. The results from qRT-PCR showed that neither *let-7* mimic nor *let-7* inhibitor affect the

mRNA expression of *Ntn1* (Fig. 2*E*). On the other hand, Western blot analysis suggested that *let-7* mimic down-regulated the protein expression of Ntn1, whereas *let-7* inhibitor up-regulated the protein expression of Ntn1 (Fig. 2*F*). Moreover, an animal model of peripheral nerve crush injury was utilized to investigate the *in vivo* effect of *let-7* agomir and *let-7* antagonist

Regulatory mechanisms of microRNAs in axon guidance

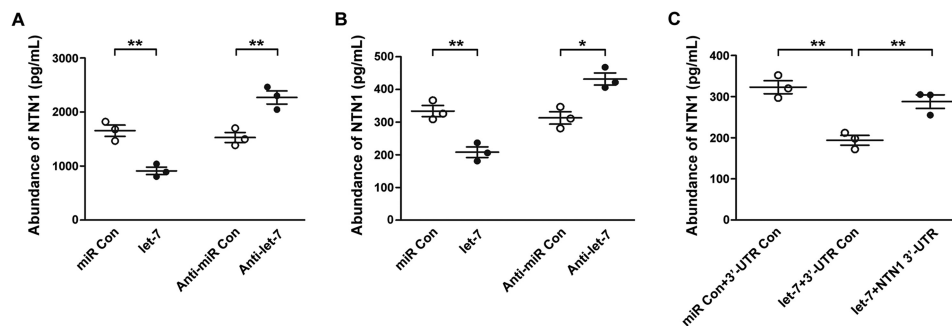


Figure 3. Effects of *let-7* on Ntn1 secretion. Primary SCs (A) and RSC96 SCs (B) were transfected with *let-7* mimic (*let-7*), *let-7* inhibitor (*Anti-let-7*), mimic control (*miR Con*), or inhibitor control (*Anti-miR Con*), respectively. The Ntn1 secretions from both primary SCs and RSC96 SCs transfected with *let-7* mimic were significantly decreased, whereas the Ntn1 secretions from both primary SCs and RSC96 SCs transfected with *let-7* inhibitor were increased significantly as compared with that transfected with the corresponding controls ($n = 3/\text{group}$). C, *let-7*-induced reduction of Ntn1 secretion was rescued by co-transfection with *let-7* mimic plus *Ntn1* 3'-UTR plasmid ($n = 3/\text{group}$). *, $p < 0.05$; **, $p < 0.01$ versus control.

on expression of the Ntn1 protein. As compared with the corresponding control group, the application of *let-7* agomir significantly decreased expression of the Ntn1 protein, whereas no significant difference was detected in the application of *let-7* antagonist (Fig. 2G). Both *in vitro* and *in vivo* results suggested that *let-7* targeted and regulated the expression of Ntn1. Furthermore, as previously obtained qRT-PCR results demonstrated, members of the *let-7* family were consistently up-regulated at day 1 and down-regulated at day 7 post-nerve as compared with the 0-h control (12). Interestingly, compared with the temporal expressions of *Ntn1* (Fig. 1A), the expression of *let-7* was correlated with that of Ntn1.

let-7 inhibited the secretion of Ntn1 from SCs

To identify the impact of *let-7* on cellular function, primary SCs and RSC96 SCs were transfected with *let-7* mimic, *let-7* inhibitor, or nontargeting negative controls. Because Ntn1 is a secreted protein, ELISA was used to determine the effects of *let-7* on the secretion of Ntn1. In the cultured primary SCs, transfection with the *let-7* mimic and *let-7* inhibitor significantly decreased and increased the secretion of Ntn1, respectively, as compared with the control (Fig. 3A). Similarly, in RSC96 SCs, *let-7* mimic and *let-7* inhibitor suppressed and elevated the secretion of Ntn1, respectively (Fig. 3B). Subsequently, RSC96 SCs were co-transfected with *let-7* mimic and *Ntn1* 3'-UTR plasmid. Consistent with these observations in Fig. 3B, *let-7* mimic induced a reduction in Ntn1 secretion. However, this effect was abolished by *Ntn1* 3'-UTR plasmid (Fig. 3C), indicating that the inhibitory effect of *let-7* on Ntn1 secretion was mediated by targeting Ntn1.

miR-9 negatively regulated *Dcc* by directly targeting its 3'-UTR

The potential regulatory miRNAs of *Dcc* were also investigated. Similar to the identification of regulatory miRNAs of *Ntn1*, candidate miRNAs of *Dcc* were discovered using TargetScan prediction software and the correlation between the expression of miRNAs and mRNAs. Among these identified miRNAs, *miR-9*, *miR-27*, *miR-128*, *miR-192*, *miR-203*, and *miR-489* were highly conserved across species and hence, selected for subsequent studies (Fig. 4A). After construction and insertion of *miR-9*, *miR-27*, *miR-128*, *miR-192*, *miR-203*,

or *miR-489* and the 3'-UTR of *Dcc* into the downstream region of the luciferase reporter gene, *miR-9* significantly reduced luciferase activity (Fig. 4B). Moreover, after the construction and insertion of *miR-9* and the WT or mutant 3'-UTR of *Dcc* into the downstream region of the luciferase reporter gene (Fig. 4C), only the plasmid containing the WT 3'-UTR of *Dcc* led to a robust reduction in luciferase activity (Fig. 4D). qRT-PCR and Western blot analysis showed that *miR-9* failed to affect the mRNA expression of *Dcc* (Fig. 4E) but distinctly affected the protein expression (Fig. 4, F and G). Furthermore, the *in vivo* effect of *miR-9* was explored in a rat model of sciatic nerve crush. Western blot analysis suggested that *miR-9* agomir and *miR-9* antagonist suppressed and elevated the protein expression of *Dcc*, respectively (Fig. 4, H and I). Also, the expression pattern of *miR-9* after sciatic nerve crush was negatively correlated with that of *Dcc* (Fig. 4J). These results demonstrated that *miR-9* directly bound to *Dcc* and regulated its expression.

miR-9 and *Dcc* affected SC migration

Transwell migration assay was conducted to observe the effect of *miR-9* and *Dcc* on modulation of the phenotype of cultured primary SCs. Compared with the SCs transfected with nontargeting negative control, transfection with *miR-9* mimic or *miR-9* inhibitor induced a significant decrease or increase in the rate of cell migration, respectively (Fig. 5A). Then, the SCs were transfected with *Dcc* siRNA that stably reduced *Dcc* expression (Fig. 5, B and C). Similar to the effect of *miR-9* mimic, *Dcc* siRNA reduced the migration rate of SCs (Fig. 5D). Moreover, co-transfection of *Dcc* siRNA with the *miR-9* inhibitor abrogated the effect of the *miR-9* inhibitor partially, indicating that *miR-9* affects the migration of SCs by targeting *Dcc* (Fig. 5E).

let-7 and *miR-9* inhibit the expression of Ntn1 and *Dcc* in dorsal root ganglions neurons (DRGs) and suppress the axon outgrowth

In addition to SCs, we also tested whether *let-7* and *miR-9* could target *Ntn1* and *Dcc* in neuron cells by transfecting the mimic or inhibitor of *let-7* and *miR-9* in the DRGs. Western blotting assay showed that *let-7* and *miR-9* mimics inhibited the expression of Ntn1 and *Dcc* proteins, whereas *let-7* and *miR-9* inhibitors promoted the expression of the proteins (Fig. 6, A

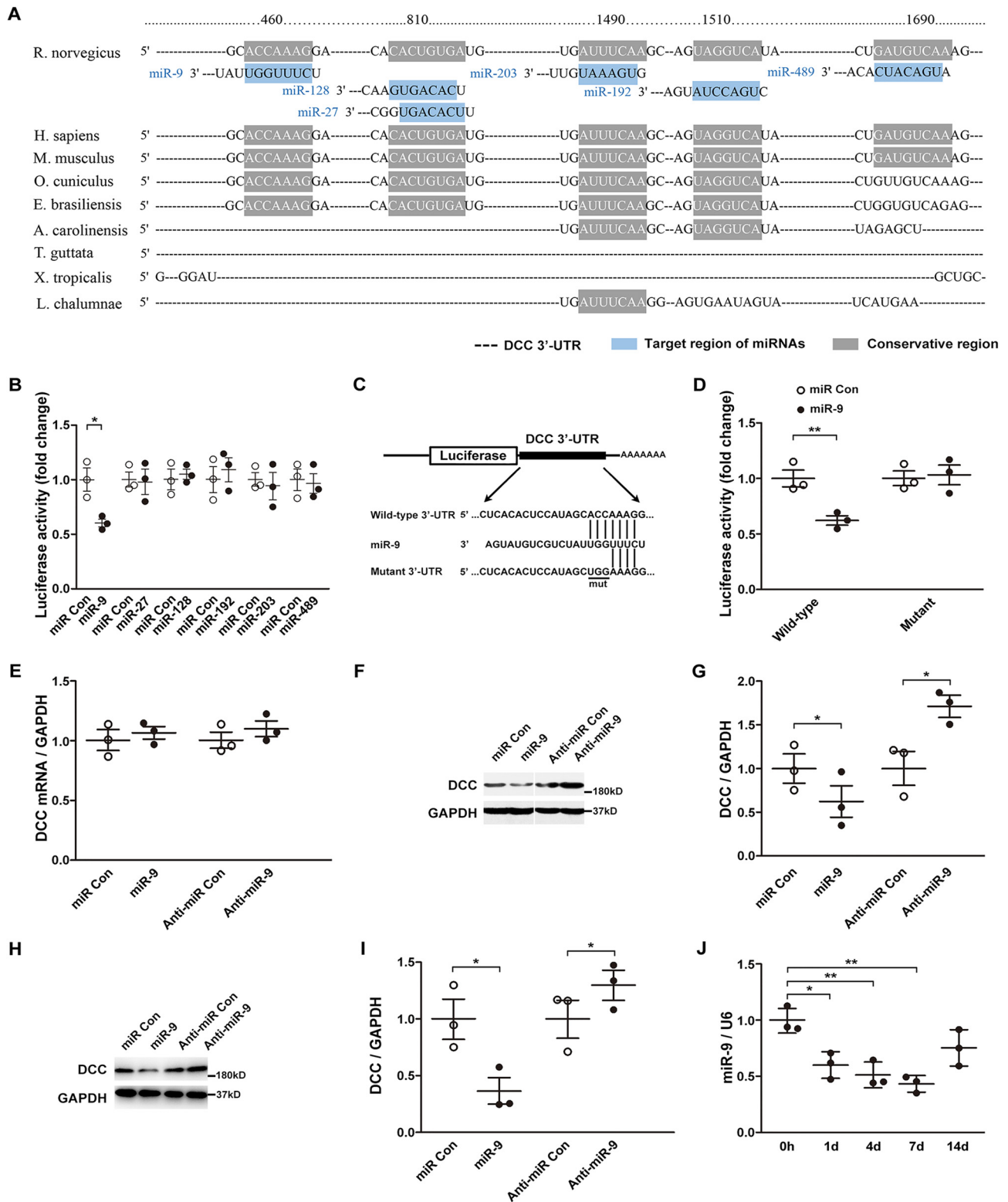


Figure 4. Identification of potential regulatory miRNAs targeting *Dcc*. *A*, cross-species conservation of binding to target *Dcc* 3'-UTR for *miR-9*, *miR-27*, *miR-128*, *miR-192*, *miR-203*, and *miR-489*. *B*, relative luciferase activities of 293T cells transfected with *miR-9* mimic (*miR-9*), *miR-27* mimic (*miR-27*), *miR-128* mimic (*miR-128*), *miR-192* mimic (*miR-192*), *miR-203* mimic (*miR-203*), *miR-489* mimic (*miR-489*), and mimic control (*miR Con*) ($n = 3$ /group). *C*, sketches of the construction of WT or mutant *p-Luc-UTR* vectors for *miR-9*. *D*, the relative luciferase activities of 293T cells transfected with WT or mutant *p-Luc-UTR* and *miR-9* mimic (*miR-9*) or mimic control (*miR Con*) ($n = 3$ /group). *E*, the mRNA expressions of *Dcc* in SCs transfected with *miR-9* mimic (*miR-9*) and mimic control (*miR Con*) or with *miR-9* inhibitor (*Anti-miR-9*) and inhibitor control (*Anti-miR Con*) ($n = 3$ /group). *F* and *G*, the protein expressions of *Dcc* in SCs transfected with *miR-9* mimic (*miR-9*) and mimic control (*miR Con*) or with *miR-9* inhibitor (*Anti-miR-9*) and inhibitor control (*anti-miR Con*) ($n = 3$ /group). *H* and *I*, the protein expressions of *Dcc* in injury sciatic nerve stumps was due to receiving an injection of a mixture containing *miR-9* agomir (*miR-9*) and agomir control (*miR Con*) or with *miR-9* antagonist (*Anti-miR-9*) and antagonist control (*Anti-miR Con*), respectively ($n = 3$ /group). *J*, the temporal expression pattern of *miR-9* in the injured nerve stumps after sciatic nerve injury ($n = 3$ /group). *, $p < 0.05$ and **, $p < 0.01$ versus control.

Regulatory mechanisms of microRNAs in axon guidance

and B). Immunohistochemistry showed that after transfection with *let-7* or *miR-9* mimics, axon outgrowth was remarkably reduced in DRGs. Conversely, axon outgrowth was enhanced in DRGs after transfecting with *let-7* and *miR-9* inhibitor (Fig. 6, C and D).

A collaborative regulatory network of *Ntn1* and *Dcc*

A previous study showed that Src activation triggers NF- κ B activation, which in turn, directly activates Lin28 transcription and rapidly reduces the *let-7* expression (32). *miR-9* was regarded as a negative regulator of Lin28 (33). Also, *Dcc* deletion severely reduces the Src activation (34, 35). These results suggested a putative regulatory pathway between NF- κ B, Lin28, *Ntn1*, *Dcc*, and Src and implied that *let-7* and *miR-9* might be involved in this regulatory pathway. To test this hypothesis, we transfected SCs with *let-7* and found that *let-7* elevated the expression of *miR-9* and inhibited the expression of *Ntn1*, *Dcc*, Src, and NF- κ B proteins (Fig. 7A). Similarly, transfection with *Lin28* siRNA elevated the expressions of *let-7* and *miR-9* genes and reduced the expression of *Ntn1*, *Dcc*, Src, and NF- κ B proteins (Fig. 7B). These preliminary results showed that *miR-9* and *let-7* target *Dcc* and *Ntn1*, respectively, and are also linked with Src, NF- κ B, and Lin28.

Discussion

Peripheral nerves exhibited a specific ability to regrow after injury. However, patients with severe peripheral nerve injury often showed poor nerve regeneration and incomplete functional recovery (36). The failure of functional recovery might be attributed to the termination of the growth of axons that do extend accurately into the corresponding effector tissues. The accurate pathfinding of the growing axons is guided by diffusible or bound factors that attract or repel the axonal growth cones (37). *Ntn1* and its receptor *Dcc* play essential roles in axon guidance. The current study investigated the expression patterns of *Ntn1* and *Dcc*, and found that the expressions were altered after sciatic nerve injury. Also, *Ntn1* and *Dcc* might be involved in peripheral nerve injury and regeneration.

miRNAs are critical post-transcriptional regulators that participate in axonal navigation in the central nervous system (4, 38–40), the proliferation and migration of SCs, and the axonal growth of neurons in the peripheral nervous system (11–14). Furthermore, this study showed that miRNAs might also regulate axon guidance in the peripheral nervous system. Target prediction algorithm and conservative analysis suggested that *Ntn1* and *Dcc* might be potential target genes of *let-7* and *miR-9* miRNAs. The data from the luciferase reporter assay confirmed that *let-7* and *miR-9* directly targeted the 3'-UTR of *Ntn1* and *Dcc*, respectively. Also, we observed that *let-7* and *miR-9* regulated the *Ntn1* and *Dcc* expression independently *in vitro* and *in vivo*, as well as that *Ntn1* and *Dcc* were real target genes of *let-7* and *miR-9*, respectively.

Specifically, *Ntn1* protein is secreted into the extracellular environment and plays a guiding role in axon guidance after nerve injury. The current study showed that *let-7* affected the amount of secreted *Ntn1* from SCs, and thus, affect axon guidance via binding of *Ntn1* to its receptor *Dcc* in the axons. Therefore, we tested the effect of *miR-9* on the expressions of *Dcc* in

DRGs. Western blotting results indicated that *miR-9* altered the expression of *Dcc* in DRGs, indicating that *miR-9* regulated axon guidance by targeting *Dcc* in DRGs.

Axon outgrowth and axon guidance are two critical aspects in nerve development and regeneration with indivisible correlation, therefore, we observed the influence of *let-7* and *miR-9* on the axon outgrowth of DRGs. The results showed that the *let-7* and *miR-9* mimics decreased the axon outgrowth, whereas it was increased by *let-7* and *miR-9* inhibitors. These results were consistent with those described in a previous study (40–43).

Previously, we reported that after sciatic nerve injury, differentially expressed *let-7* and *miR-1* regulated the SC phenotype, such as proliferation and migration by targeting NGF and BDNF independently and further influenced the axon growth of sciatic nerve (12, 13). Interestingly, *miR-340* targets and regulates the tPA such as to affect the debris clearance and the axon growth (14). The current study identified that *let-7* and *miR-9* were regulatory miRNAs of *Ntn1* and *Dcc*, and therefore the addition of *let-7* and *miR-9* to a regulatory network ensured that damaged axons proliferated in the correct direction. Also, we systematically explored the miRNA-mediated regulation of axon growth (*let-7* and *miR-1*), debris clearance (*miR-340*), and axon guidance (*let-7* and *miR-9*) by the corresponding targets NGF, BDNF, tPA, *Ntn1*, and *Dcc*. Some studies reported that *Ntn1*, *Dcc*, Src, NF- κ B, and Lin28 formed a complex regulatory pathway (32–35, 44). Combined with our previous and current works, a regulation schematic diagram can be summarized in Fig. 8. It clearly clarifies the regulation pathway with Lin28, *let-7*, and *miR-9* as the core regulation center (Fig. 8).

Debris removal, axonal growth, and axon guidance are three key elements that contribute to peripheral nerve regeneration. Following nerve injury, SCs, undergoing dedifferentiation/proliferation and migration help to improve the regenerative microenvironment by the removal of myelin debris, secretion of several factors, and formation of Bungner band (45, 46). The injured axon is triggered by intrinsic regenerative abilities. The current results showed that these miRNAs in the regulatory network controlled the regenerative microenvironment of the injured nerves and affected further nerve regeneration. These findings would aid in understanding the complex regulatory mechanisms during peripheral nerve injury and regeneration. However, additional comprehensive studies are essential for an in-depth perspective on these molecular mediators, coupled with the related bioprocesses and signaling pathways, are orchestrated to activate the intrinsic regenerative programs of peripheral nerves. Thus, the present study not only provides an insight into miRNA regulation of peripheral nerve regeneration but also opens a novel therapeutic avenue for the repair of peripheral nerve injury by regulating the production of *Ntn1* and *Dcc*.

Experimental procedures

Animal surgery and tissue preparation

Sprague-Dawley rats were purchased from the Experimental Animal Center of Nantong University, Nantong, Jiangsu,

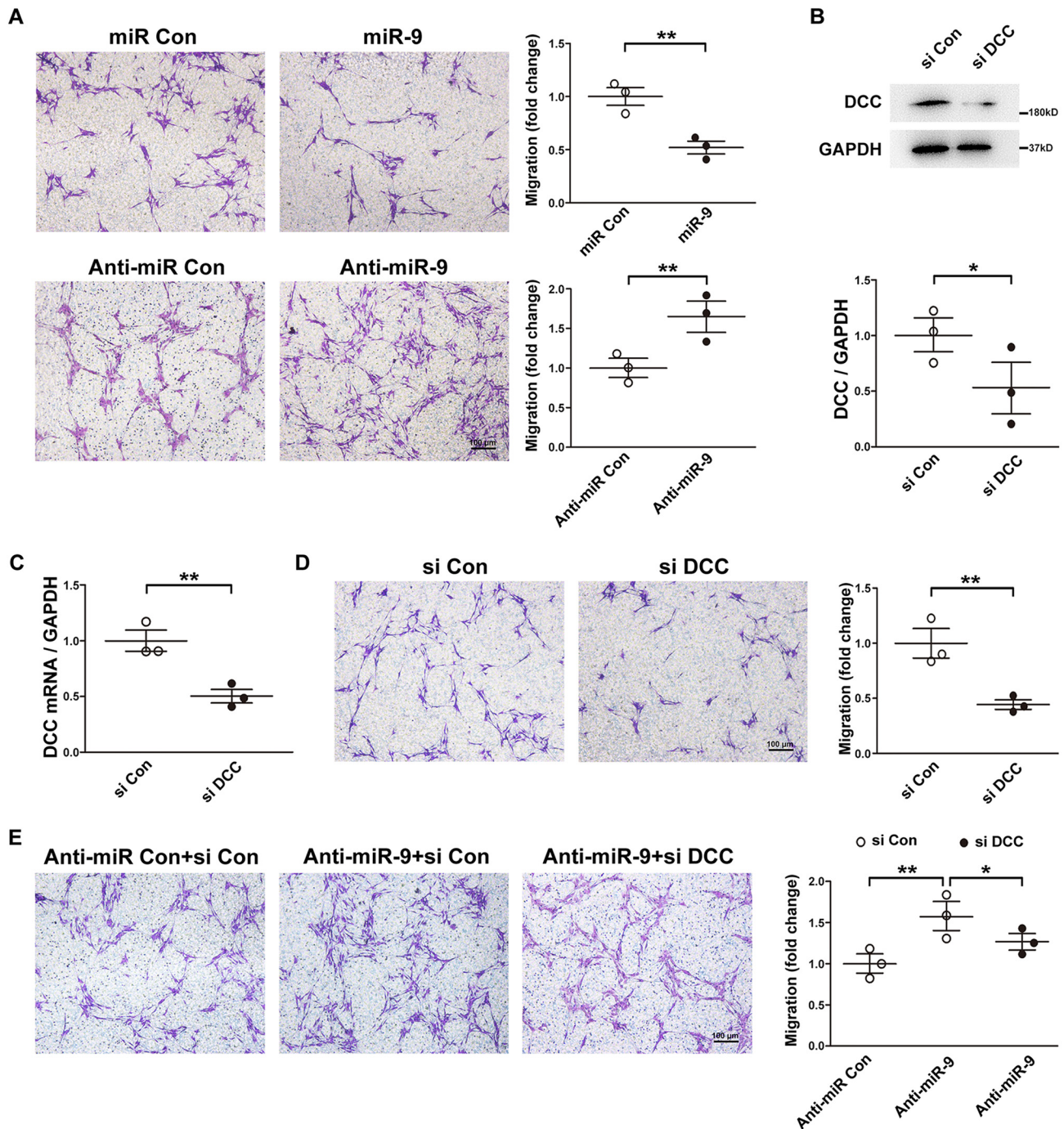


Figure 5. Effect of *miR-9* and *Dcc* on SC migration. *A*, images showing that primary SCs migrated to the bottom of the Transwell chamber after transfection with *miR-9* mimic (*miR-9*), *miR* Con, *miR-9* inhibitor (*Anti-miR-9*), and anti-*miR* Con, respectively. Dot plots showing the cell migration ability (normalized to control) of transfected SCs, $n = 3/\text{group}$, scale bar = 100 μm . *B*, the *Dcc* protein expression, and *C*, the *Dcc* mRNA expression in primary SCs were decreased by transfection with *Dcc* siRNA (*si DCC*), respectively ($n = 3/\text{group}$). *D*, the migration ability of primary SCs was decreased by *Dcc* siRNA (*si DCC*), $n = 3/\text{group}$, scale bar = 100 μm . *E*, an increase in the cell migration of SCs transfected with *miR-9* inhibitor (*Anti-miR-9*) was partially rescued by cotransfection with *Dcc* siRNA (*si DCC*) ($n = 3/\text{group}$, scale bar = 100 μm). *, $p < 0.05$ and **, $p < 0.01$ versus control.

China. All experimental and animal handling procedures were executed according to the Institutional Animal Care Guidelines of Nantong University and all animal experiments were ethically approved by the Administration Committee of Experimental Animal, Jiangsu, China.

Adult, male Sprague-Dawley rats (180–220 g) were anesthetized with intraperitoneal injection of complex narcotics (85 mg/kg of trichloroacetaldehyde monohydrate, 42 mg/kg of

magnesium sulfate, and 17 mg/kg of sodium pentobarbital). Rat sciatic nerve was exposed through an incision on the lateral aspect of the mid-thigh of the left hind limb. A 3-mm long segment of sciatic nerve was crushed two times (15 s each time with a 3-s interval) using a pair of hemostatic forceps. To minimize the discomfort and possible painful mechanical stimulation, the rats were housed in large cages with sawdust bedding post-surgery. The crushed sciatic nerve with both nerve ends

Regulatory mechanisms of microRNAs in axon guidance

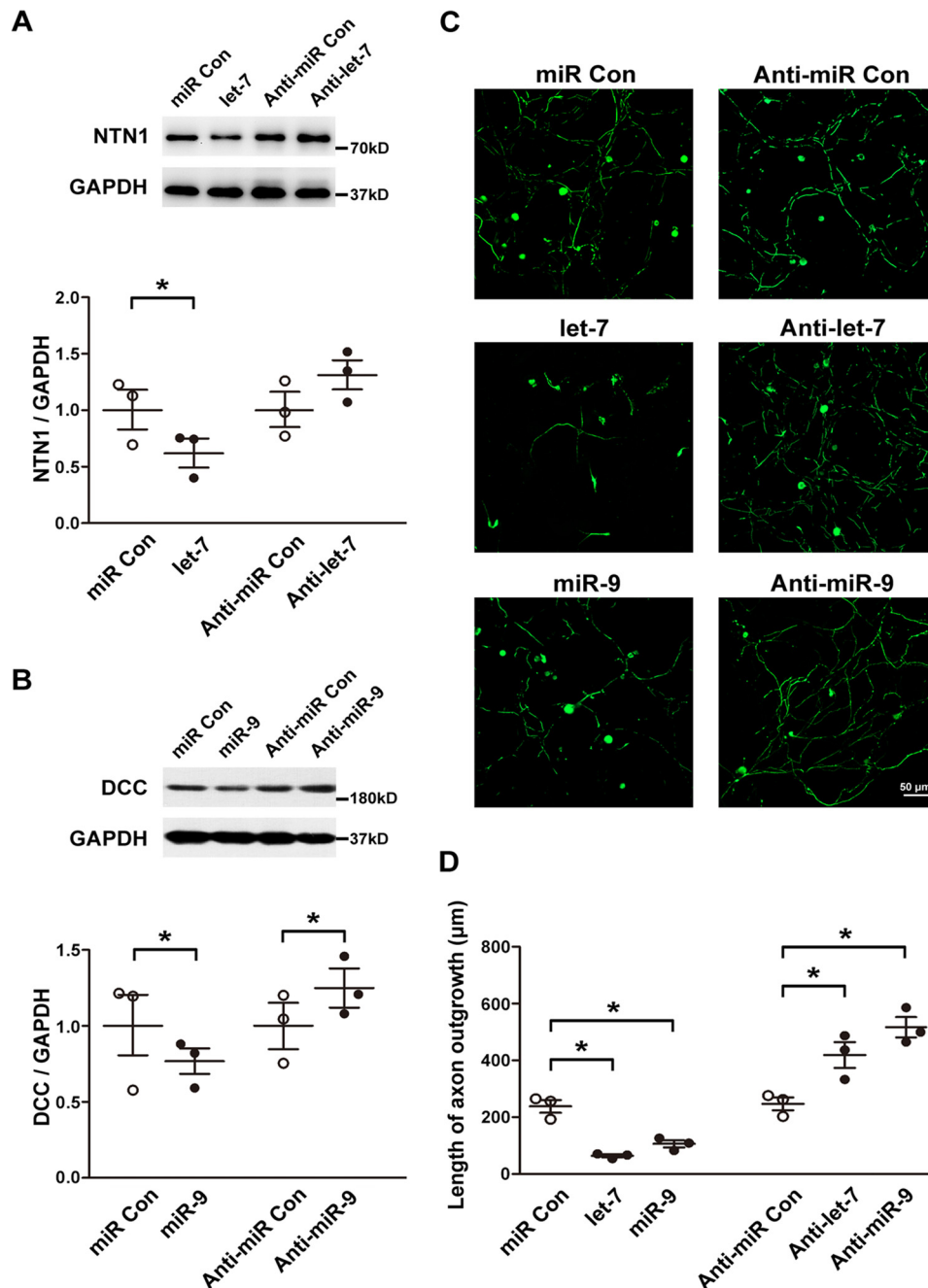


Figure 6. Effect of *let-7* and *miR-9* on the expression of Ntn1 and Dcc and axon outgrowth in DRGs. *A*, the protein expressions of Ntn1 in DRGs transfected with *let-7* mimic (*let-7*) and mimic control (*miR Con*) or with *let-7* inhibitor (*Anti-let-7*) and inhibitor control (*Anti-miR Con*), respectively ($n = 3$ /group). *B*, the protein expressions of Dcc in DRGs transfected with *miR-9* mimic (*miR-9*) and mimic control (*miR Con*) or with *miR-9* inhibitor (*Anti-miR-9*) and inhibitor control (*Anti-miR Con*), respectively ($n = 3$ /group). *C*, immunostaining with anti-NF200 showing that axon outgrowth was decreased in DRGs, which was transfected with *let-7* mimic (*let-7*) and *miR-9* mimic (*miR-9*). On the other hand, the axon outgrowth was increased in DRGs, which was transfected with *let-7* inhibitor (*Anti-let-7*) and *miR-9* inhibitor (*Anti-miR-9*). Scale bar = 50 μ m. *D*, the average length of axon outgrowth in DRGs ($n = 3$ /group). *, $p < 0.05$ versus control.

(1-mm long) was harvested at 0 h and on days 1, 4, 7, and 14 after nerve crush.

For *in vivo* experiments, the crush site was injected with a mixture (a volume ratio of 1:1) of Matrigel (BD Biosciences, Billerica, MA) and miRNA agomir, miRNA antagomir, or the corresponding controls (Ribobio, Guangzhou, China), respectively. On day 3 post-surgery, the sciatic nerve segments together with both nerve ends (1-mm long) were collected for subsequent Western blot analysis to determine the protein expression levels of Ntn1 and Dcc.

Cell culture and transfection

Primary SCs were collected from the sciatic nerves of 1-day-old postnatal Sprague-Dawley rats and further isolated from the fibroblasts using anti-Thy1.1 antibody and rabbit complement (Sigma) as described previously (12). The purity of SCs was assessed by immunostaining with anti-S100 (DAKO, Carpinteria, CA). The primary SCs or RSC96 SCs (American Type Culture Collection) were cultured in Dulbecco's modified Eagle's medium (DMEM) containing 10% fetal bovine serum at 37 $^{\circ}$ C in a humidified incubator with 5% CO₂.

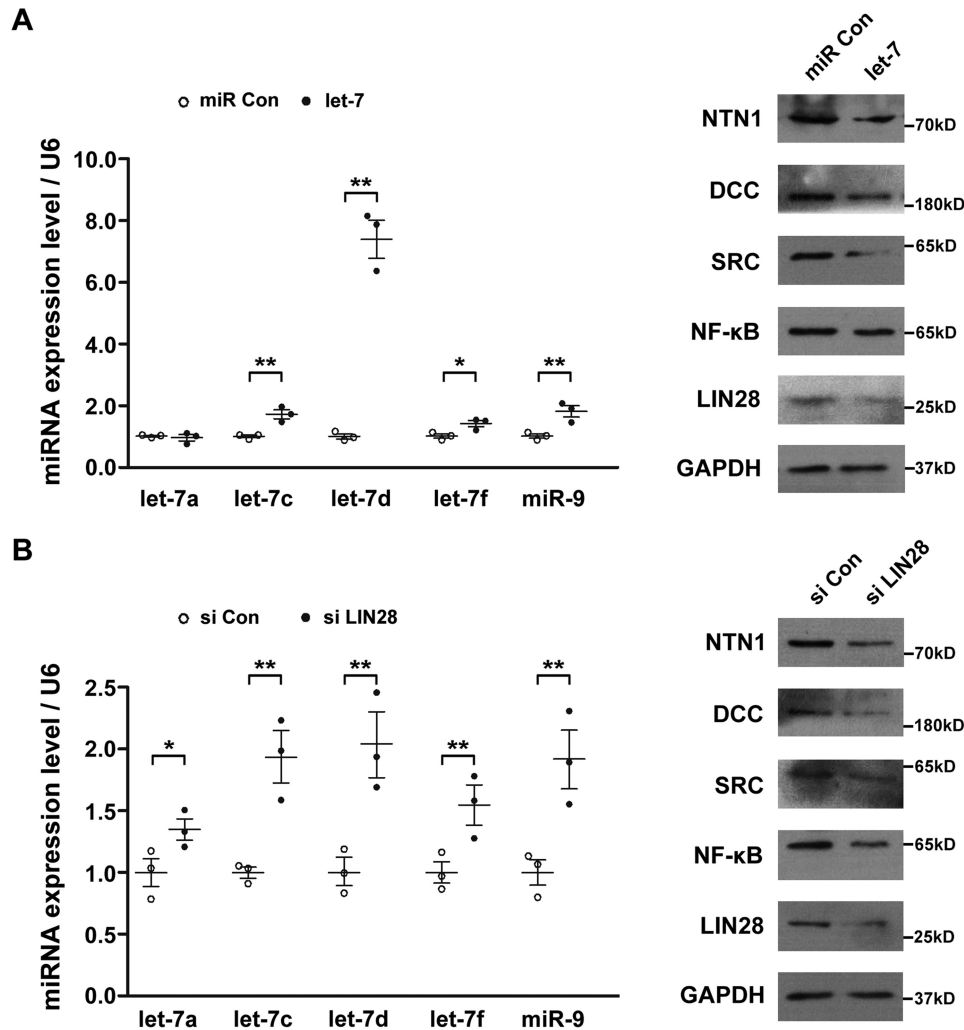


Figure 7. Regulatory network of Ntn1 and Dcc. *A*, the effect of *let-7* mimic (*let-7*) transfection on the expressions of *let-7* and *miR-9* genes and that of Ntn1, Dcc, Src, NF- κ B, and Lin28 proteins ($n = 3/\text{group}$). *B*, the effect of *Lin28* siRNA (*si Lin28*) transfection on the expressions of *let-7* and *miR-9* genes and that of Ntn1, Dcc, Src, NF- κ B, and Lin28 proteins ($n = 3/\text{group}$). *, $p < 0.05$ and **, $p < 0.01$ versus control.

DRGs were removed from 1-day-old postnatal Sprague-Dawley rats and digested in 1% collagenase type I (Sigma) for 30 min at 37 °C, and 0.25% trypsin (Invitrogen) for 10 min, followed by mechanically triturated using a pipette to obtain single cell suspension. Subsequently, the cells were centrifuged at 900 rpm for 10 min on 15% BSA (Sigma) in PBS (Invitrogen) to remove the SCs. Purified DRGs were cultured on poly-L-lysine-coated glass plates in Neurobasal (Invitrogen) and B-27 (Invitrogen). Cultured cells were transfected with miRNA mimics, miRNA inhibitors, or the corresponding controls (Ribobio) using Lipofectamine RNAiMAX transfection reagent (Invitrogen) according to the manufacturer's instructions.

qRT-PCR

Total RNA was extracted using TRIzol (Life Technologies) according to the manufacturer's instructions. The contaminating DNA was removed using RNeasy spin columns (Qiagen, Valencia, CA). The quality of the isolated RNA samples was evaluated using an Agilent Bioanalyzer 2100 (Agilent Technologies, Santa Clara, CA) and the quantity of RNA samples was determined using a NanoDrop ND-1000 spectrophotometer

(Infinigen Biotechnology Inc., City of Industry, CA). An equivalent of 20 ng of RNA samples was reversely transcribed using TaqMan MicroRNA Reverse Transcription Kit (Applied Biosystems, Foster City, CA) and stem-loop RT primers (Ribobio) according to the manufacturer's instructions to determine the miRNA expression. The mRNA was reverse transcribed into cDNA using a Prime-Script Reagent Kit (TaKaRa, Dalian, China) according to the manufacturer's instructions. qRT-PCR was performed using SYBR Green Premix Ex Taq (TaKaRa) with *Ntn1* and *Dcc* primers on an Applied Biosystems StepOne real-time PCR system to evaluate the mRNA expression of the corresponding genes. The sequences of primers were as follows (5'–3'): *Ntn1*, forward, GCAGCATGGAAGAACCCTGA and reverse, CGGCGTATACGACTTGTGC; *Dcc*, forward, ACAACAGGGAGCGAGCTTT and reverse, GCAGATACAGCGTGCAGGT; *Gapdh*, forward, CCTTCATTGACCTCAACTACATG and reverse, CTTCTCCATGGTGGTGAAGAC. The reactions were carried out in triplicate. The relative expressions of miRNAs and mRNAs were calculated using the comparative $2^{-\text{rrCt}}$ method; *U6* and *Gapdh* served as the reference genes, respectively.

Regulatory mechanisms of microRNAs in axon guidance

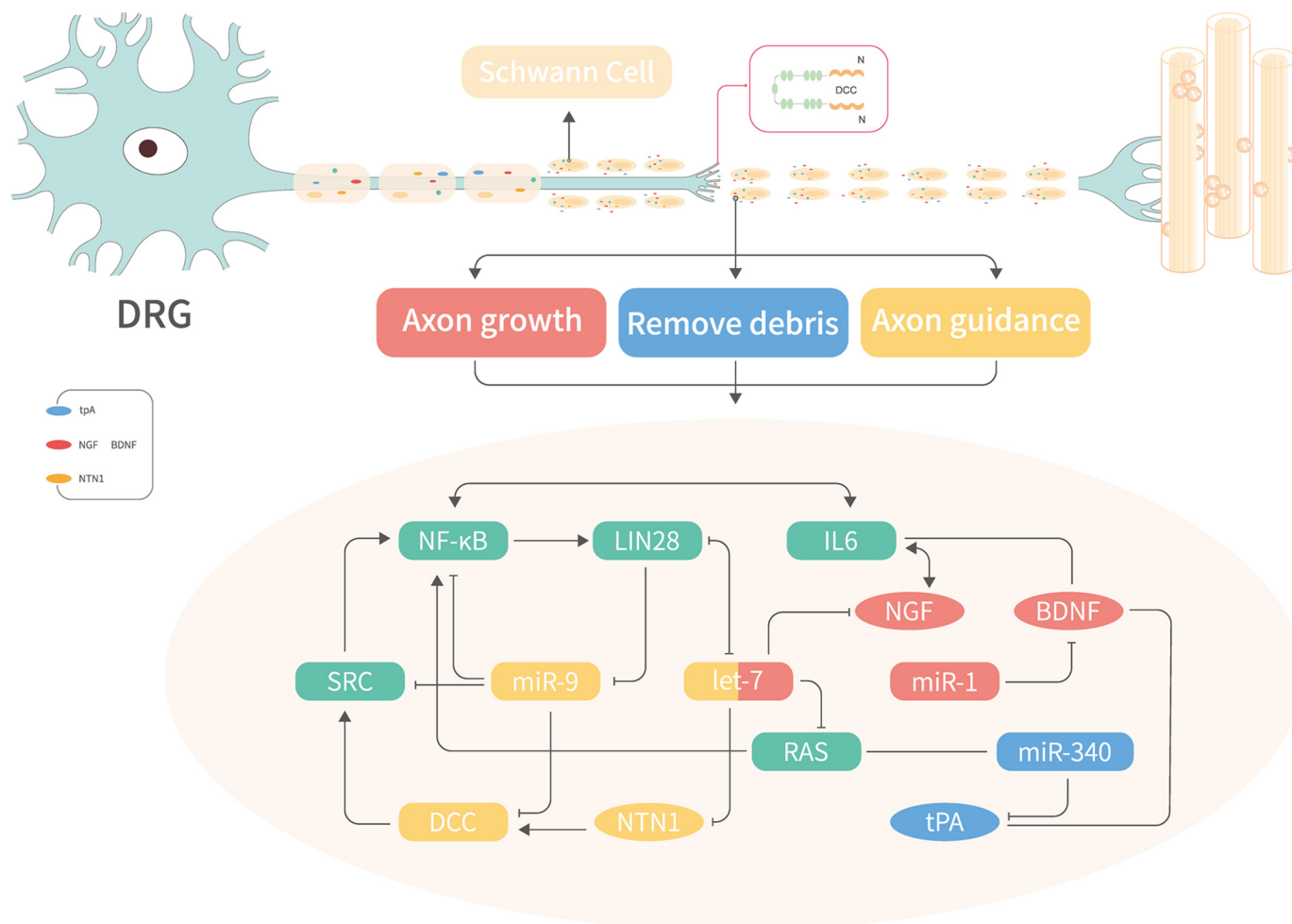


Figure 8. Schematic representation of axon growth, debris clearance, axon guidance, and correlated miRNA regulatory network during peripheral nerve regeneration.

Western blot analysis

Protein extracts were prepared from nerve tissues. Equivalent amounts of isolated protein were separated on 10% SDS-PAGE and transferred to polyvinylidene difluoride membranes (Millipore, Bedford, MA). Then, these membranes were blocked with 5% nonfat dry milk in Tris-HCl–buffered saline (TBS) at room temperature and probed with Ntn1 (1:1000, Abcam, Cambridge, MA) and Dcc (1:2000, Santa Cruz Biotechnology, Santa Cruz, CA) primary antibodies, followed by horseradish peroxidase-conjugated second antibody. Subsequently, the membrane was developed with enhanced chemiluminescence reagent (Cell Signaling, Beverly, MA) and exposed to Kodak X-Omat Blue film (PerkinElmer Life Sciences, Boston, MA). The immunoreactive bands were analyzed quantitatively using Grab-it 2.5 and Gelwork software.

Cell migration assay

The migration of SCs was examined using 6.5-mm Transwell chambers with 8- μ m pores (Costar, Cambridge, MA). The bottom surface of each membrane was coated with 10 μ g/ml of fibronectin. An equivalent of 10^6 cells/ml of SCs in 100 μ l of DMEM was transferred to the top chambers of each Transwell and allowed to migrate at 37 °C in a 5% CO₂ incu-

bator. A volume of 600 μ l of complete medium was injected into the lower chambers. The upper surface of each membrane was cleaned with a cotton swab at the indicated time points. The cells adhering to the bottom surface of each membrane were stained with 0.1% crystal violet, imaged, and enumerated using a DMR inverted microscope (Leica Microsystems, Bensheim, Germany). The assays were repeated three times in triplicate.

Plasmid construction and luciferase assay

The luciferase reporter vector was constructed by transferring the fragment of luciferase from pGL3-Basic vector using HindIII and XbaI and inserting a multiple cloning sequence after the XbaI site in the pcDNA3 vector. The 3'-UTR of *Ntn1* or *Dcc* was amplified from the genomic DNA by PCR and subcloned into the region directly downstream of the stop codon in the luciferase gene in the luciferase reporter vector to generate *p-Luc-UTR* reporter plasmid. Then, overlap PCR was used to construct the 3'-UTR mutant reporter plasmid. The primers used to generate the WT, and mutant 3'-UTRs were as follows (5'-3'): *Ntn1* 3'-UTR, forward, TCCGGTACCCAGGCCCTGGAGAAATGA and reverse, GGGTCTAGACAAGGTTCTCAAGAGACAAG; *Ntn1* 3'-UTR mutant, forward, GCGCCG-

TGACCAAGCTATGTCTTGTCATTT and reverse, GAC-ATAGCTTGGTCACGGCGCTCCTTCCAG; *Dcc* 3'-UTR, forward, CGGAATTCATGCATTGCCAAACCGTT-GAG and reverse, CCGCTCGAGGCCCAAATATTGAACA-AAAG; *Dcc* 3'-UTR mutant, forward, GAAAACATCCA-ATCCTTTCAGCTATGGAG and reverse, ACTCTCAC-ACTCCATAGCTGGAAAGGATTG. The sequences of WT and mutant 3'-UTR were confirmed by sequencing.

For luciferase assay, HEK 293T cells were seeded in 24-well plates and transfected with a mixture of 120 ng of *p*-Luc-UTR, 20 pmol of miRNA mimic, and 20 ng of *Renilla* luciferase vector pRL-CMV (Promega, Madison, WI) using the Lipofectamine 2000 transfection system (Invitrogen). The luciferase activity was measured from the cell lysate at 24 h post-transfection using the Dual-Luciferase Reporter Assay System according to the recommended protocols (Promega).

ELISA

Primary SCs and RSC96 SCs were transfected with 10 nM *let-7* mimic, 40 nM *let-7* inhibitor, and the corresponding dose negative controls, respectively, using Lipofectamine RNAiMAX transfection reagent (Invitrogen). For reverse analysis, RSC96 SCs were transfected using the Lipofectamine 2000 transfection system (Invitrogen) with miRNA mimic control and vector control plasmid, *let-7* mimic and vector control plasmid, or *let-7* mimic and *Ntn1* 3'-UTR plasmid. Subsequently, primers used to amplify the *Ntn1* 3'-UTR fragment were as follows (5'-3'): forward, TCCGGTACCCAGGCC-TGGAGAAATGA and reverse, TCCGGTACCTAACCATCAAATACAGTG. Then, the *Ntn1* 3'-UTR fragment was cloned into the pcDNA3 to construct the *Ntn1* 3'-UTR plasmid, whereas the empty pcDNA3 vector served as the control. An equivalent of 6 μ g of plasmid was added in a well of 6-well plate, whereas the concentration of *let-7* mimic was 10 nM. The fetal bovine serum-free DMEM was replaced, and the reaction incubated for an additional 48 h. Finally, the medium was collected and passed through a 0.22- μ m filter (Millipore) to obtain the supernatant that was concentrated to an appropriate volume by freeze-drying. The protein levels of Ntn1 were measured using a Ntn1 enzyme-linked immunosorbent assay (ELISA) kit (Molecular Innovations, Novi, MI). The data from 3 independent cultures, each comprising of triplicate wells, were collected and expressed as an averaged.

Immunohistochemistry

DRGs were fixed in 4% paraformaldehyde after culturing for 48 h and immunostained with mouse anti-neurofilament 200 (1:500, Sigma) primary antibody, followed by the fluorescent-labeled secondary antibodies (1:400, Invitrogen). Images were acquired by fluorescence microscopy (Leica). The experiment was repeated three times.

Statistical analysis

The Student's *t* test or analysis of variance was used for statistical analysis conducted on SPSS 15.0 software (SPSS, Chicago, IL). *p* < 0.05 was considered statistically significant. All data were expressed as mean \pm S.E.

Author contributions—X. W. and S. L. resources; X. W., Q. C., S. Y., Q. L., R. Z., P. W., T. Q., and S. L. data curation; X. W., Q. C., S. Y., Q. L., R. Z., and P. W. software; X. W., Q. C., S. Y., Q. L., R. Z., P. W., T. Q., and S. L. formal analysis; X. W. and S. L. supervision; X. W. and S. L. funding acquisition; X. W. and S. L. validation; X. W., Q. C., S. Y., Q. L., R. Z., and S. L. methodology; X. W., Q. C., S. Y., Q. L., and S. L. writing-original draft; X. W., Q. C., S. Y., Q. L., R. Z., and S. L. writing-review and editing.

References

- Gaudet, A. D., Popovich, P. G., and Ramer, M. S. (2011) Wallerian degeneration: gaining perspective on inflammatory events after peripheral nerve injury. *J. Neuroinflammation* **8**, 110 [CrossRef Medline](#)
- Wu, D., and Murashov, A. K. (2013) Molecular mechanisms of peripheral nerve regeneration: emerging roles of microRNAs. *Front. Physiol.* **4**, 55 [Medline](#)
- Cheng, X. L., Wang, P., Sun, B., Liu, S. B., Gao, Y. F., He, X. Z., and Yu, C. Y. (2015) The longitudinal epineural incision and complete nerve transection method for modeling sciatic nerve injury. *Neural Regen. Res.* **10**, 1663–1668 [CrossRef Medline](#)
- Iyer, A. N., Bellon, A., and Baudet, M. L. (2014) microRNAs in axon guidance. *Front. Cell Neurosci.* **8**, 78 [Medline](#)
- da Silva, T. F., Eira, J., Lopes, A. T., Malheiro, A. R., Sousa, V., Luoma, A., Avila, R. L., Wanders, R. J., Just, W. W., Kirschner, D. A., Sousa, M. M., and Brites, P. (2014) Peripheral nervous system plasmalogen regulate Schwann cell differentiation and myelination. *J. Clin. Invest.* **124**, 2560–2570 [CrossRef Medline](#)
- Giraldez, A. J., Mishima, Y., Rihel, J., Grocock, R. J., Van Dongen, S., Inoue, K., Enright, A. J., and Schier, A. F. (2006) Zebrafish miR-430 promotes deadenylation and clearance of maternal mRNAs. *Science* **312**, 75–79 [CrossRef Medline](#)
- Bagga, S., Bracht, J., Hunter, S., Massirer, K., Holtz, J., Eachus, R., and Pasquinelli, A. E. (2005) Regulation by *let-7* and *lin-4* miRNAs results in target mRNA degradation. *Cell* **122**, 553–563 [CrossRef Medline](#)
- Piao, X., Zhang, X., Wu, L., and Belasco, J. G. (2010) CCR4-NOT deadenylates mRNA associated with RNA-induced silencing complexes in human cells. *Mol. Cell. Biol.* **30**, 1486–1494 [CrossRef Medline](#)
- Flamand, M. N., Wu, E., Vashisht, A., Jannot, G., Keiper, B. D., Simard, M. J., Wohlschlegel, J., and Duchaine, T. F. (2016) Poly(A)-binding proteins are required for microRNA-mediated silencing and to promote target deadenylation in *C. elegans*. *Nucleic Acids Res.* **44**, 5924–5935 [CrossRef Medline](#)
- Djuranovic, S., Nahvi, A., and Green, R. (2012) miRNA-mediated gene silencing by translational repression followed by mRNA deadenylation and decay. *Science* **336**, 237–240 [CrossRef Medline](#)
- Zhou, S., Gao, R., Hu, W., Qian, T., Wang, N., Ding, G., Ding, F., Yu, B., and Gu, X. (2014) miR-9 inhibits Schwann cell migration by targeting Cthrc1 following sciatic nerve injury. *J. Cell Sci.* **127**, 967–976 [CrossRef Medline](#)
- Li, S., Wang, X., Gu, Y., Chen, C., Wang, Y., Liu, J., Hu, W., Yu, B., Wang, Y., Ding, F., Liu, Y., and Gu, X. (2015) *Let-7* microRNAs regenerate peripheral nerve regeneration by targeting nerve growth factor. *Mol. Ther.* **23**, 423–433 [CrossRef Medline](#)
- Yi, S., Yuan, Y., Chen, Q., Wang, X., Gong, L., Liu, J., Gu, X., and Li, S. (2016) Regulation of Schwann cell proliferation and migration by miR-1 targeting brain-derived neurotrophic factor after peripheral nerve injury. *Sci. Rep.* **6**, 29121 [CrossRef Medline](#)
- Li, S., Zhang, R., Yuan, Y., Yi, S., Chen, Q., Gong, L., Liu, J., Ding, F., Cao, Z., and Gu, X. (2017) miR-340 regulates fibrinolysis and axon regrowth following sciatic nerve injury. *Mol. Neurobiol.* **54**, 4379–4389 [CrossRef Medline](#)
- Li, S., Qian, T., Wang, X., Liu, J., and Gu, X. (2017) Noncoding RNAs and their potential therapeutic applications in tissue engineering. *Engineering* **3**, 3–15 [CrossRef](#)

Regulatory mechanisms of microRNAs in axon guidance

16. Kefeli, U., Ucuncu Kefeli, A., Cabuk, D., Isik, U., Sonkaya, A., Acikgoz, O., Ozden, E., and Uygun, K. (2017) Netrin-1 in cancer: potential biomarker and therapeutic target. *Tumour Biol.* **39**, 1010428317698388 [Medline](#)
17. Mediero, A., Wilder, T., Ramkhalawon, B., Moore, K. J., and Cronstein, B. N. (2016) Netrin-1 and its receptor Unc5b are novel targets for the treatment of inflammatory arthritis. *FASEB J.* **30**, 3835–3844 [CrossRef](#) [Medline](#)
18. Wang, X., Xu, J., Gong, J., Shen, H., and Wang, X. (2013) Expression of netrin-1 and its receptors, deleted in colorectal cancer and uncoordinated locomotion-5 homolog B, in rat brain following focal cerebral ischemia reperfusion injury. *Neural Regen. Res.* **8**, 64–69 [Medline](#)
19. Poliak, S., Morales, D., Croteau, L. P., Krawchuk, D., Palmesino, E., Morton, S., Cloutier, J. F., Charron, F., Dalva, M. B., Ackerman, S. L., Kao, T. J., and Kania, A. (2015) Synergistic integration of Netrin and ephrin axon guidance signals by spinal motor neurons. *Elife* **4**, e10841 [CrossRef](#) [Medline](#)
20. Cai, Y., Hu, C. J., Wang, J., and Wang, Z. H. (2011) Influence of deleted in colorectal carcinoma gene on proliferation of ovarian cancer cell line SKOV-3 *in vivo* and *in vitro*. *Chin. Med. Sci. J.* **26**, 175–181 [CrossRef](#) [Medline](#)
21. Geisbrecht, B. V., Dowd, K. A., Barfield, R. W., Longo, P. A., and Leahy, D. J. (2003) Netrin binds discrete subdomains of DCC and UNC5 and mediates interactions between DCC and heparin. *J. Biol. Chem.* **278**, 32561–32568 [CrossRef](#) [Medline](#)
22. Keleman, K., and Dickson, B. J. (2001) Short- and long-range repulsion by the *Drosophila* Unc5 netrin receptor. *Neuron* **32**, 605–617 [CrossRef](#) [Medline](#)
23. Hamasaki, T., Goto, S., Nishikawa, S., and Ushio, Y. (2001) A role of netrin-1 in the formation of the subcortical structure striatum: repulsive action on the migration of late-born striatal neurons. *J. Neurosci.* **21**, 4272–4280 [CrossRef](#) [Medline](#)
24. Moon, C., Kim, H., Ahn, M., Jin, J. K., Wang, H., Matsumoto, Y., and Shin, T. (2006) Enhanced expression of netrin-1 protein in the sciatic nerves of Lewis rats with experimental autoimmune neuritis: possible role of the netrin-1/DCC binding pathway in an autoimmune PNS disorder. *J. Neuroimmunol.* **172**, 66–72 [CrossRef](#) [Medline](#)
25. Yi, S., Zhang, H., Gong, L., Wu, J., Zha, G., Zhou, S., Gu, X., and Yu, B. (2015) Deep sequencing and bioinformatic analysis of lesioned sciatic nerves after crush injury. *PLoS ONE* **10**, e0143491 [CrossRef](#) [Medline](#)
26. Yi, S., Tang, X., Yu, J., Liu, J., Ding, F., and Gu, X. (2017) Microarray and qPCR analyses of Wallerian degeneration in rat sciatic nerves. *Front. Cell Neurosci.* **11**, 22 [Medline](#)
27. Bosse, F., Hasenpusch-Theil, K., Küry, P., and Müller, H. W. (2006) Gene expression profiling reveals that peripheral nerve regeneration is a consequence of both novel injury-dependent and reactivated developmental processes. *J. Neurochem.* **96**, 1441–1457 [CrossRef](#) [Medline](#)
28. Liu, S., Yin, F., Zhang, J., Wicha, M. S., Chang, A. E., Fan, W., Chen, L., Fan, M., and Li, Q. (2014) Regulatory roles of miRNA in the human neural stem cell transformation to glioma stem cells. *J. Cell. Biochem.* **115**, 1368–1380 [CrossRef](#) [Medline](#)
29. Marler, K. J., Suetterlin, P., Dopplapudi, A., Rubikaite, A., Adnan, J., Maiorano, N. A., Lowe, A. S., Thompson, I. D., Pathania, M., Bordey, A., Fulga, T., Van Vactor, D. L., Hindges, R., and Drescher, U. (2014) BDNF promotes axon branching of retinal ganglion cells via miRNA-132 and p250GAP. *J. Neurosci.* **34**, 969–979 [CrossRef](#) [Medline](#)
30. Li, S., Yu, B., Wang, Y., Yao, D., Zhang, Z., and Gu, X. (2011) Identification and functional annotation of novel microRNAs in the proximal sciatic nerve after sciatic nerve transection. *Sci. China Life Sci.* **54**, 806–812 [CrossRef](#) [Medline](#)
31. Li, S., Liu, Q., Wang, Y., Gu, Y., Liu, D., Wang, C., Ding, G., Chen, J., Liu, J., and Gu, X. (2013) Differential gene expression profiling and biological process analysis in proximal nerve segments after sciatic nerve transection. *PLoS ONE* **8**, e57000 [CrossRef](#) [Medline](#)
32. Iliopoulos, D., Hirsch, H. A., and Struhl, K. (2009) An epigenetic switch involving NF- κ B, Lin28, Let-7 microRNA, and IL6 links inflammation to cell transformation. *Cell* **139**, 693–706 [CrossRef](#) [Medline](#)
33. Faria, A. M., Sbiera, S., Ribeiro, T. C., Soares, I. C., Mariani, B. M., Freire, D. S., de Sousa, G. R., Lerario, A. M., Ronchi, C. L., Deutschbein, T., Wakamatsu, A., Alves, V. A., Zerbini, M. C., Mendonca, B. B., Frago, M. C., Latronico, A. C., Fassnacht, M., and Almeida, M. Q. (2015) Expression of LIN28 and its regulatory microRNAs in adult adrenocortical cancer. *Clin. Endocrinol.* **82**, 481–488 [CrossRef](#)
34. Horn, K. E., Glasgow, S. D., Gobert, D., Bull, S. J., Luk, T., Girgis, J., Tremblay, M. E., McEachern, D., Bouchard, J. F., Haber, M., Hamel, E., Krimpenfort, P., Murai, K. K., Berns, A., Doucet, G., Chapman, C. A., Ruthazer, E. S., and Kennedy, T. E. (2013) DCC expression by neurons regulates synaptic plasticity in the adult brain. *Cell Rep.* **3**, 173–185 [CrossRef](#) [Medline](#)
35. O'Donnell, M. P., and Bashaw, G. J. (2013) Src inhibits midline axon crossing independent of Frazzled/Deleted in colorectal carcinoma (DCC) receptor tyrosine phosphorylation. *J. Neurosci.* **33**, 305–314 [CrossRef](#) [Medline](#)
36. Yao, C., Wang, Y., Zhang, H., Feng, W., Wang, Q., Shen, D., Qian, T., Liu, F., Mao, S., Gu, X., and Yu, B. (2018) lncRNA TNXA-PS1 modulates Schwann cells by functioning as a competing endogenous RNA following nerve injury. *J. Neurosci.* **38**, 6574–6585 [CrossRef](#) [Medline](#)
37. Hong, K., Nishiyama, M., Henley, J., Tessier-Lavigne, M., and Poo, M. M. (2000) Calcium signalling in the guidance of nerve growth by netrin-1. *Nature* **403**, 93–98 [CrossRef](#) [Medline](#)
38. Giraldez, A. J., Cinalli, R. M., Glasner, M. E., Enright, A. J., Thomson, J. M., Baskerville, S., Hammond, S. M., Bartel, D. P., and Schier, A. F. (2005) MicroRNAs regulate brain morphogenesis in zebrafish. *Science* **308**, 833–838 [CrossRef](#) [Medline](#)
39. Han, L., Wen, Z., Lynn, R. C., Baudet, M. L., Holt, C. E., Sasaki, Y., Bassell, G. J., and Zheng, J. Q. (2011) Regulation of chemotropic guidance of nerve growth cones by microRNA. *Mol. Brain* **4**, 40 [CrossRef](#) [Medline](#)
40. Shibata, M., Nakao, H., Kiyonari, H., Abe, T., and Aizawa, S. (2011) MicroRNA-9 regulates neurogenesis in mouse telencephalon by targeting multiple transcription factors. *J. Neurosci.* **31**, 3407–3422 [CrossRef](#) [Medline](#)
41. Basu, A., Dey, S., Puri, D., Das Saha, N., Sabharwal, V., Thyagarajan, P., Srivastava, P., Koushika, S. P., and Ghosh-Roy, A. (2017) let-7miRNA controls CED-7 homotypic adhesion and EFF-1-mediated axonal self-fusion to restore touch sensation following injury. *Proc. Natl. Acad. Sci. U.S.A.* **114**, E10206–E10215 [CrossRef](#) [Medline](#)
42. Dajas-Bailador, F., Bonev, B., Garcez, P., Stanley, P., Guillemot, F., and Papalopulu, N. (2012) MicroRNA-9 regulates axon extension and branching by targeting Map1b in mouse cortical neurons. *Nat. Neurosci.* [10.1038/nm.3082](#) [CrossRef](#) [Medline](#)
43. Jiang, J., Hu, Y., Zhang, B., Shi, Y., Zhang, J., Wu, X., and Yao, P. (2017) MicroRNA-9 regulates mammalian axon regeneration in peripheral nerve injury. *Mol. Pain* **13**, 1744806917711612 [Medline](#)
44. Bazzoni, F., Rossato, M., Fabbri, M., Gaudiosi, D., Mirolo, M., Mori, L., Tamassia, N., Mantovani, A., Cassatella, M. A., and Locati, M. (2009) Induction and regulatory function of miR-9 in human monocytes and neutrophils exposed to proinflammatory signals. *Proc. Natl. Acad. Sci. U.S.A.* **106**, 5282–5287 [CrossRef](#) [Medline](#)
45. Namgung, U. (2014) The role of Schwann cell-axon interaction in peripheral nerve regeneration. *Cells Tissues Organs* **200**, 6–12 [Medline](#)
46. Bosse, F. (2012) Extrinsic cellular and molecular mediators of peripheral axonal regeneration. *Cell Tissue Res.* **349**, 5–14 [CrossRef](#) [Medline](#)